ARGON ION POLLUTION OF THE MAGNETOSPHERE

Ramon E. Lopez
Rice University
Houston, Texas 77251

Construction of a Solar Power Satellite (SPS) would require the injection of large quantities of propellant to transport material from Low Earth Orbit (LEO) to the construction site at Geostationary Earth Orbit (GEO). This injection, in the form of $\sim 10^{32}$, 2 KeV argon ions (and associated electrons) per SPS, is comparable to the content of the plasmasphere ($\sim 10^{31}$ ions). In addition to the mass deposited, this represents a considerable injection of energy.

The injection is examined in terms of a simple model for the expansion of the beam plasma. General features of the subsequent magnetospheric convection of the argon are also examined.

INTRODUCTION

In recent years a large scale energy system, the Satellite Power System (SPS), has received considerable attention from the scientific and technical community. The basic concept for SPS is as follows: Large (10 km × 5 km) platforms would be constructed in geostationary earth orbit (GEO) to collect solar energy. This energy would be converted into microwaves and beamed down to Earth, received by a rectifying antenna and fed into the power grid.

In 1978, Rockwell International did a system definition study (ref. 1) in which a 5 GW (at Earth interface) reference system was developed. The transportation component would mandate the construction of several reusable heavy lift launch vehicles (HLLV) to haul material into low Earth orbit (LEO). From LEO the cargo would be shuttled to the construction site GEO in a fleet of electric orbit transfer vehicles (EOTV).

The EOTVs would be solar powered and propelled by argon ion thrusters. Ion thrusters have some advantages over chemical rockets. They can deliver a sustained, steady thrust. Also, the ion thruster propellant velocity is much greater than for chemical thrusters, therefore much less mass need be injected to move an equal amount of cargo from LEO to GEO with ion thrusters.

In spite of the great efficiency of ion propulsion, due to the great mass that must be transported, enormous quantities of energetic argon and the associated (thermal) electrons would be injected into the environment. Such a large scale injection of plasma into the magnetosphere is likely to have a global impact on Earth's magnetospheric morphology and dynamics. In addition, due to the highly anisotropic velocity distribution of the argon, this represents a considerable injection of free energy. Numerous processes should transfer a large portion of the

injection energy to the magnetospheric system.

Ion thruster technology is still developing and so the parameters for the thruster in question are uncertain. The Rockwell reference system described an EOTV propelled by an ion thruster with a grid potential limit of 2 keV, to avoid arcing to the background plasma. It would operate with an ion beam current of 1904 amps, have a radius $\approx$ 38 cm, and develop 69.7 Nt of thrust. Eighty such thrusters would equip each EOTV, in four groups of 20, with 16 active and 4 spares.

The thruster produces two distinct plasmas: the beam plasma and the thermal plasma produced by charge exchange between the beam plasma and escaping un-ionized argon. The number of charge-exchange ions produced per second is given by Kaufmann (ref. 2) to be:

$$\dot{N} = \frac{2\sigma_{CE} J_B^2 (1 - \eta)}{e^2 V_0 R_B \pi \eta} \quad (Ar^+ \ s^{-1})$$

(1-1)

where σ_{CE} = charge exchange cross section = 2×10^{-19} m^2
J_B = beam current = 1904 A
$\overline{V}_0$ = $(8KT/\pi m)^{1/2}$
R = beam radius = .38 m
η = fraction of propellant ionized

Carruth and Brady (ref. 3) state that in experiments with a 900-series, Hughes mercury ion thruster approximately 90% of the propellant is ionized. The remaining 10% escapes through the optics in the form of neutral mercury. Therefore η is assumed to be 0.9 and KT $\approx$ 10 eV (ref. 4), which gives $\dot{N}$ = 6.07 $\times 10^{20}$ Ar$^+$ s^{-1}. This represents about 5.6% of the beam current.

Parks and Katz (ref. 5), and Carruth and Brady (ref. 3) report that laboratory tests show the charge-exchange plasma near the thruster moves radially outward from the thruster beam. This thermal plasma will be injected into space with essentially the EOTV's orbital velocity. As in the barium release experiments (ref. 6), the plasma is expected to expand until $\beta \approx 1$, at which point the expansion perpendicular to $\vec{B}$ is stopped by the field.

This thermal argon plasma, apart from the beam plasma, would be in itself a considerable addition to the thermal heavy ion population, especially in the plasmasphere. The remaining un-ionized argon would be subject to charge exchange and photoionization, the latter of which has an e-folding production rate given by Siscoe and Mukherjee (ref. 7) to be 4.5 $\times$ 10^{-4} s^{-1}. This allows many of the fast (charge-exchange) neutrals to escape, while trapping the thermal neutrals in, or near, the plasmasphere.

TABLE I. — SPS PARAMETERS

SPS mass $\sim$ 5 $\times$ 10^7 Kg
EOTV — LEO departure $\sim$ 6.7 $\times$ 10^6 Kg
      Cargo $\sim$ 5 $\times$ 10^6 Kg
      Propellant $\sim$ 5.5 $\times$ 10^5 Kg
LEO $\rightarrow$ GEO $\rightarrow$ LEO trip time $\approx$ 130 days

The quantities of mass involved in the reference system are given in table I. To build a 5 GW station of a mass $\approx 5 \times 10^7$ Kg, one needs ≈ 10 EOTV flights which would inject 5×10^6 Kg of 2 keV Ar^+ and $\sim 5 \times 10^5$ Kg of thermal Ar^+ (along with the associated electrons) into the magnetosphere. Assuming that two stations are built per year this gives an average injection rate of 5.3×10^{26} Ar^+ s^{-1}. This is comparable to the polar wind injection rate of $\sim 3 \times 10^{26}$ s^{-1} and equal to the plasma sheet loss rate (ref. 8). The average rate of energy injection (in the form of 2 keV Ar^+) is $\sim 10^9$ watts, while an average substorm deposites 10^{11}-10^{12} watts into the ionosphere (ref. 9). This energy will, however, be distributed over a smaller area and so power densities could be similar to auroral power densities.

Needless to say, the scope of the questions involved in such an injection is extensive. This paper will concern itself mainly with two topics: the injection of the energetic ions (beam plasma dynamics) and the subsequent convection of the beam ions in the magnetosphere.

BEAM PLASMA DYNAMICS

The plasma beam that emerges from the thruster is a dense, charge-neutral beam moving perpendicular to $\vec{B}$. The physics of a plasma beam injected into a transverse magnetic field has been studied by many authors, both experimentally and theoretically (refs. 10, 11, 12, 13). Also there have been authors who have considered the problem of ion thrusters in space, some specifically in the SPS context (refs. 4, 14, 15).

Curtis and Grebowsky (ref. 14) argue that the beam polarizes and $\vec{E} = -\vec{V} \times \vec{B}$ cancels the Lorentz force. According to Curtis and Grebowsky (ref. 14) the beam density is always able to support the polarization field. In this case the beam simply passes out of the magnetosphere, depositing a thin non-propagating sheath. While this is correct for a vacuum injection, when the field lines threading the beam are shorted the plasma is stopped (refs. 10, 13). This is exactly the case in the magnetosphere. The beam dynamics paradigm of Chiu et al. (ref. 15) is based on the barium release experiments (refs. 6, 12). In this picture the polarization field accelerates and polarizes the adjacent plasma, which in turn polarizes the plasma adjacent to it. This electric field, which moves along the field line at the Alfvén speed, transfers beam momentum to the ambient plasma and magnetosphere. When the Alfven wave reaches the ionosphere it drives dissipative Pedersen currents, and can be partially reflected (ref. 6).

According to this model the plasma velocity decreases like $e^{-t/\tau}$, where τ is the amount of time it takes for the Alfvén wave to travel over as much mass per unit area as is causing the disturbance. Therefore, Chiu et al. (ref. 15) give that

$$\tau = \int dz \, \rho_b / 2 V_A \rho_0 \qquad (2-1)$$

where ρ is the mass density (b refers to the beam, 0 to the ambient), V_A is the Alfvén speed, and the integral is along the field line. Calculations using realistic plasmaspheric and magnetic field models, give $\tau \approx 10$ seconds (ref. 16). Thus the beam can travel for distances ≤ 1000 km.

Treumann et al. (ref. 17) have pointed out that as field aligned currents short out the polarization field, electrons cannot $\vec{E} \times \vec{B}$ drift across field lines to neu-

tralize the beam. They postulate that more currents parallel to $\vec{B}$ neutralize the beam head, generating a kinetic Alfvén wave. For the PORCUPINE ion beam (of which more will be said), Treumann et al. (ref. 17) estimate electron drift velocities ~V_A. Due to these high drifts they argue that anomalous heating of electrons energizes them to ~20 eV to explain those hot electrons seen in the PORCUPINE experiment (ref. 18).

If we assume that the beam width is on the order of 10 km and the beam length ~1000 km then the average neutralizing field-aligned currents (for the EOTV discussed above) must be ~16 $\mu A/m^2$. For ambient electron densities of $\lesssim 10^9$ m^{-3} this results in drift speeds $\gtrsim 100$ km s^{-1}. This is still half the thermal speed of a 0.1 eV electron, so ion acoustic waves will be stable, but electrostatic ion-cyclotron waves, with $w = \Omega_i$, are unstable for $V_D \gtrsim 5 \times$ (ion thermal speed) (ref. 19) thus limiting the current. Therefore it is unlikely that the polarization field will be completely shorted out and that the beam ions will be charge-neutralized by a combination of both $\vec{E} \times \vec{B}$ drift of beam electrons across $\vec{B}$ and field-aligned currents.

Haerendal and Sagdeev (ref. 8), writing on behalf of the PORCUPINE experimenters, report on the injection of a 4A, 200 eV, Xe^+, charge-neutralized plasma beam. This beam was injected at ~72° to $\vec{B}$ in nine events ranging in altitude from 196 km to 451 km. They report three stages of its beam expansion. The first is free expansion of the beam until the magnetic pressure starts to balance the dynamic pressure. The second phase is one of diffusive expansion, with the polarization field allowing for some motion across $\vec{B}$, although the polarization field is rapidly shorted out by field-aligned currents and the beam is stopped. The third phase is that of single particle motion.

Considerable wave activity was also reported during the injection events (refs. 18, 20, 21). Broadband ion-cyclotron harmonic waves were detected (refs. 18, 21) and it has been argued that the Drummond-Rosenbluth instability (ref. 19) is responsible (ref. 18). Given the much greater scale of the SPS injection it is reasonable to expect intense wave generation which could energize ambient particles. In particular there is experimental evidence for the acceleration of thermal electrons by ion-cyclotron waves. Norris et al. (ref. 22) suggest that these waves in the magnetosphere having $f > f_{He^+}$ accelerate electrons with a clear bias parallel to $\vec{B}_0$, the majority of the electrons heated to 20 eV.

The field-aligned currents produced as a result of this are consistent with the view that such currents will play a central role in the dynamics of the beam, since these currents transfer momentum from the beam and drive Alfvén waves. This is supported by observations of considerably enhanced electron fluxes during the injection of a plasma transverse to $\vec{B}$ as reported by Alexandrov et al. (ref. 23). These authors also suggest that the observed magnetic disturbances are due to field-aligned currents and associated Alfvén waves.

The beam model presented below will deal with only the large-scale dynamics of the beam. It is assumed that the paradigm of Scholer (ref. 6) is essentially correct, so beam velocity decreases as $e^{-t/\tau}$. When the beam emerges from the thruster both nkT and $(1/2)\rho v^2$ are much greater than $B^2/2\mu_0$. Thus the beam will expand radially outward from the beam axis, as if into a vacuum, forming a cone. This phase of the expansion continues until

$$nKT \simeq B^2/2\mu_0 \qquad (2-2)$$

after which motion perpendicular to $\vec{V}_B$ and $\vec{B}$ is stopped, while expansion along the field line continues essentially uninhibited (fig. 1). The beam travels in this manner until

$$\frac{1}{2} \rho v^2 \simeq B^2/2\mu_0 \tag{2-3}$$

at which point the geomagnetic field becomes the dominant influence in the argon plasma's motion. The argon's subsequent motion can then be followed by the adiabatic theory.

In the initial phase of the plasma beam we are dealing with a vacuum expansion. It is assumed the beam is charge-neutral and collisionless. In the very early history of the beam it is certainly collisional, the plasma rapidly thermalizing, but by ~100 m downstream the mean free path is of the order of the beam size. We also neglect momentum loss to Alfvén waves, assuming $t \ll \tau$ during the first (vacuum) phase of the beam expansion.

To represent the plasma that emerges from the thruster we write

$$f(\vec{X}, \vec{Y}, V_z, t = 0) = \frac{n_0 m}{2\pi KT} \delta(V_z - V_B) \exp -\left[\frac{m\vec{V}^2}{2KT} + \frac{\vec{X}^2}{2R^2}\right] \tag{2-4}$$

where
$$\vec{X} = X\hat{i} + Y\hat{j}$$
$$\vec{V} = V_x\hat{i} + V_y\hat{j}$$
$$\vec{V}_B = \text{beam velocity} \equiv V_B\hat{z}$$
$$R = 1/3\ r_0$$

Liemohn et al. (ref. 4) give $KT \simeq 10$ eV, which for a 2 keV beam gives an effective beam divergence angle ~8°. This same 8° spreading angle is reported by Cybulski et al. (ref. 24) in flight tests of the SERT I ion thruster. To confine the plasma to the thruster at $t = 0$, R is set to one-third the thruster radius, r_0.

We can then write the collisionless, vacuum Boltzman equation

$$\frac{\partial f}{\partial t} + \vec{V} \cdot \nabla f = 0 \tag{2-5}$$

The solution to equation (2-5) is readily found to be

$$f(\vec{X}, \vec{V}, V_z, t) = \frac{n_0 m}{2\pi KT} \delta(V_z - V_B) \exp -\left[\frac{m\vec{V}^2}{2KT} + \frac{(\vec{X} - \vec{V}t)^2}{2R^2}\right] \tag{2-6}$$

The constant, n_0, is given by the normalization condition

$$\int f d^2v\ d\vec{x}\ V_B t = N = \frac{It}{e} \tag{2-7}$$

where the integral along the beam axis is replaced by multiplication by $V_B t$. From equation (2-7) one finds

$$n_0 = \frac{9I}{2\pi r_0^2 eV_B} \tag{2-8}$$

The density of ions is given by

$$\int f \, d^3v = n(\vec{x}, t) = n_0 \frac{m/KT}{(m/KT) + (t^2/R^2)} \exp\left[- \frac{\dot{X}^2}{2R^2} \frac{m/KT}{(m/KT) + (t^2/R^2)}\right] \quad (2\text{-}9)$$

which for $t \gtrsim 10^{-4}$ s yields, using equation (2-8)

$$n(r, t) = \frac{m}{KT} \frac{I}{2\pi e V_B t^2} \exp\left[- \frac{r^2}{2t^2} \frac{m}{KT}\right] \quad (2\text{-}10)$$

The end of the vacuum expansion phase is given by equation (2-2) using equation (2-10) evaluated at the edge of the beam, which is $r \simeq V_{Th} t$. The time at which this condition is satisfied for the EOTV in question in a dipole field is

$$t_0 = 8.83 \times 10^{-3} L^3 \text{ sec} \quad (2\text{-}11)$$

where L is the magnetic shell parameter. After time t_0 the beam continues to spread along $\vec{B}$ and so the density decreases like $1/t$. But the velocity is also going down as $e^{-t/\tau}$ and so the density must go like $e^{t/\tau}$ to conserve particles. So we may write the central beam density for $t > t_0$ as

$$n(t > t_0) = \frac{t_0 n(r = 0, t = t_0)}{t} e^{-t/\tau} \quad (2\text{-}12)$$

Using this density in equation (2-3) yields an equation for the time of transition from beam motion to adiabatic motion, which is

$$L^3 = 0.216 \, t \, e^{t/\tau} \quad (2\text{-}13)$$

where L is the dipole shell parameter. The fraction of energy the beam ions retain is then $e^{-2t/\tau}$, the rest of the energy being transferred to the magnetosphere and ionosphere. As stated before, $\tau \simeq 10$ sec in the plasmasphere (ref. 15). Figure 2 gives the energy loss as a function of L for $\tau = 10$ sec from L = 2.5 to L = 3.5.

To estimate the energy density deposited in the ionosphere by the beam we find that at L = 2 roughly 3/4 of the beam power is lost to Alfvén waves. From equation (2-11) we find that the beam width ~ few km, and the beam length $\lesssim$ 1000 km. This gives an area of $\lesssim 10^4$ km^2, which mapped down to the ionosphere (with a dipole field) results in ionospheric power densities of ~10^{-1} W/m^2 (assuming the bulk of the energy is deposited in the ionosphere). This is considerably larger than auroral power densities of ~10^{-2} W/m^2 (ref. 25), and even if we assume only 10% of the power is absorbed by the ionosphere there would still be power densities equivalent to aurorae.

CONVECTION OF THE ARGON PLASMA

Once the argon plasma's transition from beam to individual particle motion is accomplished the subsequent motion is determined by the local magnetic and electric fields. This motion is most easily followed using the guiding center approximation. The two first order drift velocities are the $\vec{E} \times \vec{B}$ and the gradient/curvature drift

680

velocities. The motion of the plasma is given by

$$\frac{d\vec{x}}{dt} = \frac{\vec{E} \times \vec{B}}{B^2} + \frac{(1/2)\,'mv^2}{B} (1 + \cos^2 \alpha) \frac{\vec{B} \times \vec{\nabla}|\vec{B}|}{eB^2} \tag{3-1}$$

Ignoring time dependence, $\vec{E}$ and $\vec{B}$ are functions of $\vec{x}$ and this equation must be solved numerically.

The coordinate system is as follows: x is the antisunward direction, y along the dawn meridian. For a magnetic field the model of Mead (ref. 26) is used with the magnetopause set at r = 10 $R_\oplus$. In the equatorial plane, $\vec{B}$ just has a z component:

$$B = B_z = \frac{3.11 \times 10^{-5}}{R^3} + 2.515 \times 10^{-8} - 2.104 \times 10^{-9} \; R \cos \theta \tag{3-2}$$

where R is the earth radii, θ is the local time and B in tesla.

There are three components to the electic field: the convection field, the corotation field and the self-electric field of the argon plasma, which will be discussed in more detail below. The convection field is approximated by a constant, dawn to dusk, 0.2 mV/m electric field. This corresponds to a ≈ 50 kV cross-polar potential drop mapped out onto a 40 $R_\oplus$ magnetosphere. The corotation field is given by

$$\vec{E}_{cor} = -\vec{V} \times \vec{B} \; \cong \; -\vec{\Omega} \times \vec{r} \times \vec{B}_{Dipole} \tag{3-3}$$

The above model has some obvious shortcomings. The greatest of these is the assumption of a uniform convection field. In addition, there is an inconsistency in making the approximation in equation (3-3), then using it in the drift equation, since the expression for $\vec{B}$ has non-dipole components. The proper way to calculate the corotating field is to calculate $\vec{V} \times \vec{B}$ for the field line in question. This was not done due to the limitations of the Tektronics 4052 minicomputer which was used. However, this rough model should give a somewhat reasonable approximation to the general features of the convection of injected argon.

Chiu et al. (ref. 15) give the time fraction spent from LEO to GEO in figure 3. Using this with the above model one finds that ~3/4 of the injected argon is trapped in the plasmasphere. However, a more complete picture of the argon convection requires the inclusion of the electric field generated by the argon filled flux tube itself. The gradient drift current in the flux tube (or plasma blob) gives rise to Birkeland currents, which close in the ionosphere, if neighboring flux tubes cannot satisfy continuity of current. This current system is illustrated in figure 4.

Assuming that equal amounts of current go to the northern and southern hemispheres current continuity gives

$$\frac{1}{2} \nabla \cdot \vec{J}_{\perp eq} = -J_{\parallel eq} = - \left(\frac{B_{eq}}{B_{ion}} \right) J_{\parallel ion} \tag{3-4}$$

where $\vec{J}_{\perp eq}$ is the current/length in the equatorial plane, $J_{\parallel eq}$ is the current/unit

area out of the equatorial plane, and $J_{\|ion}$ the current/unit area into the ionosphere. This current closes in the ionosphere, in which case we can take the divergence of Ohm's Law and, using equation (3-4), obtain

$$\nabla \cdot (\underline{\Sigma} \cdot \nabla V) = \frac{1}{2} \nabla \cdot J_{\perp eq} \left(\frac{B_{ion}}{B_{eq}}\right) \tag{3-5}$$

Assuming $\vec{J}_{ion}$ to be $\perp \vec{B}$, and considering only the Pedersen conductivity, the above becomes

$$\Sigma_p \nabla_h^2 V = \frac{1}{2} \nabla \cdot \vec{J}_{eq} \left(\frac{B_{ion}}{B_{eq}}\right), \quad \nabla_h = \text{horizontal } \nabla \text{ in ionosphere} \tag{3-6}$$

This approach, developed in part by Vasyliunas (ref. 27) and Wolf (ref. 28), allows the calculation of the ionospheric potential set up by the flux tube. This potential can be then mapped out along field lines (assuming they are equipotentials) to give the potential, and electric field, in the equatorial plane.

We assume the argon density to be constant throughout a flux tube of radius a, and zero outside of the flux tube. It is also assumed that there is a uniform, background current density. For this case, in radial coordinates centered on the flux tube, we find

$$\nabla \cdot \vec{J}_{\perp eq} = K \cos \theta \, \delta(r - a) \tag{3-7}$$

where K is a constant. As a further simplification we assume we are dealing with a circle in a locally flat ionosphere, so equation (3-6) becomes

$$\nabla^2 V = \frac{K'}{\Sigma_p} \cos \psi \, \delta(\rho - a') \tag{3-8}$$

where (ρ, ψ) are the ionospheric coordinates whose origin is the field line threading the center of the plasma blob, and K', a' are constants. The solution is obtained in a straightforward fashion to yield, in the ionosphere

$$V = \frac{K'a'}{2\Sigma_p \rho} \cos \psi, \qquad \rho > a'$$

$$= \frac{K'\rho}{2\Sigma_p} \cos \psi, \qquad \rho < a' \tag{3-9}$$

Mapping the resultant electric field out to the equatorial plane along dipole field lines yields

$$\vec{E}_{Blob} = -\frac{K'\hat{\phi}}{2\Sigma_p \lambda^{3/2}} \tag{3-10}$$

where ϕ is local time and λ is the L shell of the center of the argon flux tube. This electric field, for negative K', results in $\vec{E} \times \vec{B}$ motion radially outwards from earth. We also note that the field outside the blob is that of a dipole.

The constant K' is related, by equations (3-6) and (3-7) to the divergence of

the net current, which is

$$\nabla \cdot \vec{J}_{1eq} = (|\vec{J}_{BG}| - |\vec{J}_{GC}|) \cos \theta \, \delta(r - a) \qquad (3-11)$$

where $|\vec{J}_{GC}|$ is the gradient-curvature current, and $|\vec{J}_{BG}|$ is the background current present in neighboring flux tubes.

We can consider two extreme cases concerning the condition of the argon in the flux tube: very strong pitch angle scattering so that the distribution is isotropic, or very weak scattering so the plasma mirrors at the equator ($\sim$ the state of injection). In the later case

$$\vec{J}_{GC} = N\mu \, \frac{\vec{B} \times \nabla\beta}{B^2} \qquad (3-12)$$

where N is the number/area and μ is the magnetic moment. To find μ one can use the beam model of Chapter 2 to obtain the ion's perpendicular energy when they start convective motion. For a dipole field this gives

$$K' = \left(|\vec{J}_{BG}| - \frac{3N\mu}{R_\oplus L}\right) \left(\frac{B_{ion}}{B_{eq}}\right) \qquad (3-13)$$

In the former case the flux tube can be treated as an ideal gas, in which case an adiabatic energy invariant λ can be defined (ref. 29)

$$E_K = \frac{\text{kinetic energy}}{\text{particle}} = \lambda \left(\int ds/B \right)^{-2/3} \qquad (3-14)$$

One can also define a number invariant (ref. 29)

$$\eta = n \int ds/B = N/B = \#/\text{flux}; \qquad \dot{n} = \#/m^3 \qquad (3-15)$$

then the gradient-curvature drift current is given by (ref. 29)

$$\vec{J}_{GC} = n\lambda\hat{z} \times \nabla_{eq} \left(\int ds/B \right)^{-2/3} \qquad (3-16)$$

Using equations (3-14) and (3-15) the above can be written

$$\vec{J}_{GC} = \varepsilon\hat{z} \times \nabla \left(\int ds/B \right) \qquad (3-17)$$

where ε is the energy density of the flux tube. This form is convenient since Williams (ref. 30) gives the quiet time energy density to be $\sim 10^{-9}$ Joules/m^3 from $L \sim 2$-5.5, thus we can calculate the background gradient-curvature drift current, $\vec{J}_{BG}$.

To proceed we need to calculate η, λ, $\int ds/B$, and $\nabla(\int ds/B)$. The flux tube volume is given by G.-H. Voigt (personal communication, 1982) to be

$$\int ds/B = \frac{2(L)^{1/2}(L-1)^{1/2}}{7B_0} \left[1 + \frac{6}{5} L + \frac{8}{5} L^2 + \frac{16}{5} L^3\right] R_\oplus \qquad (3-18)$$

the gradient of $\int ds/B$ can be obtained by straightforward differentiation of equation

(3-18). In addition, λ may be obtained by using equation (3-14) with the ion kinetic energy given by the beam model in Chapter 2.

The number invariant, η, can be obtained from equation (3-15) if N, the area number density, is known. If I is the ion beam current of the thrusters and V_{EOTV} is the orbital velocity of the vehicle then N is given by

$$N = I/(eV_{EOTV}d_T) \qquad (3-19)$$

where d_T is the extent of the flux tube in the $\hat{V} \times \hat{B}$ direction. The width of the beam is given by $d_B \sim V_{Th}t_0$, where t_0 is given by equation (2-11). This is then the size of the region confining the gyroradii of the ions, therefore

$$d_T \simeq \frac{2mV_{ion}}{eB} + d_B \qquad (3-20)$$

With the above we may now calculate the electric field generated by the argon flux tube's gradient-curvature drift for the two extreme assumptions about the pitch-angle state of the Ar^+. Suprisingly, the difference in the gradient drift velocities, and therefore currents, is only ~10%. It would seem that the total gradient-curvature drift is not overly sensitive to the pitch-angle state of the argon.

Using equations (3-10) to (3-20), equation (3-1) was numerically integrated to produce a plotted trajectory for a model argon filled flux tube. Sample trajectories are plotted in figures 5a and 5b.

In general, the early motion of the model flux tube is dominated by the self-electric field, which results in rapid, radially outward, convection of the argon.

By the time an average flux tube has expanded and cooled to the point where outside fields dominate, it has moved to the plasmapause where a storm can dislodge it. The bulk of the argon should then drift to the magnetopause. The fraction of this argon which is convected back into the tail is of some importance since this Ar^+ could become highly energized (ref. 3). Also of concern is some knowledge of the velocity-space configuration of the Ar^+ when it enters the tail, especially if the triggering mechanism for substorms is related to the ion-tearing mode instability.

Some Ar^+, which is injected at low L can remain trapped, contaminating the plasmasphere (fig. 6). However, the major feature of the convection model is that the bulk of the argon will pass out of the plasmasphere and enter the convective cycle of the magnetosphere. If we assume that ~30% of the Ar^+ comes back up the tail, then the average mass injection rate for the tail is 2.6×10^{24} Ar^+ s^{-1}. If the tail has dimensions of 5 $R_\oplus$ × 40 $R_\oplus$ × 60 $R_\oplus$, and if we assume that an argon ion is in the plasma sheet on the order of an hour, after which it is lost, then average density would be ~10^4 m^{-3}. This is smaller than the ambient density by a factor of 10-100 (ref. 9). However, the mass density could go up by as much as a factor of four, cutting the Alfvén speed by 1/2 and thus changing the time scales for dynamic phenomena in the tail.

One more point should be made concerning the motion of the argon flux tube. The electric field of the argon blob is so large that one should ask what the role of inertial drifts is in the motion of the argon. As the flux tubes accelerate

radially outward they produce an inertial drift current oppositely directed to the gradient-curvature drift current. So the flux tubes will accelerate at the rate needed to cancel the gradient-curvature current, thus satisfying continuity, until the velocity of the Ar^+ has reached is that of the $\vec{E} \times \vec{B}$ velocity of the self-electric field, at which point it will not need to accelerate to close the current.

The inertial drift current/length is

$$\vec{j}_I = - \frac{Nm\vec{a} \times \vec{B}}{eB^2} \tag{3-21}$$

where N is the equatorial area number density and m is the argon mass. Equating this to the gradient drift current and solving for $\vec{a}$, the acceleration, gives (for $B = B_0/L^3$)

$$\vec{a} = \frac{3\mu B_0}{mR_\oplus L^4} \hat{r} \tag{3-22}$$

For argon injected at L = 2 equation (3-22) yields a ~ 5 km/s^2 so within a short time $\vec{a}t \sim \vec{E}_{BLOB} \times \vec{B}/B^2$. Thus, except for the first moments of the argon drift, inertial currents need not be self-consistently included. Gravitational and centrifugal drifts may also be neglected.

CONCLUSION

We have seen that the operation of powerful ion thrusters in the SPS context (or for that matter in any space industrial project of such scale) is expected to have a wide variety of effects. Two distinct plasmas are injected: a 2 keV beam plasma and a thermal charge-exchange plasma. The thermal plasma will be a significant addition to the heavy ion content of the plasmasphere. Immediate effects of the beam injection include wideband ion-cyclotron wave generation and field-aligned heating of electrons. Alfvén waves will transfer beam momentum to the ambient plasma and ionosphere. In the ionosphere, power densities will be of the order of, or bigger than natural auroral power densities and so the EOTV will in effect create an artificial aurora on the order of 10^2 km long. These induced aurorae will probably have localized, disruptive effects on communications, and could also affect power transmission lines (ref. 32).

Once the beam ions start to convect, they move radially outward until the argon flux tube energy density is equal to the background energy density. Therefore most of the argon will convect out of the plasmasphere. The field-aligned currents generated could cause further ionospheric disturbances. The argon will then enter the general convective cycle and be distributed throughout much of the magnetosphere. This significant number of heavy ions could substantially alter dynamic quantities like the Alfvén speed. The dispersion relation for waves would also be altered. New cutoffs and resonances should appear along with new wave-particle phenomena. In fact, Chiu et al. (ref. 15) have shown that the presence of Ar^+ damps the instability which precipitates MeV electrons, therefore those levels should rise.

Thus, we see that the operation of an argon-ion propelled orbital transfer system will substantially modify the magnetosphere-ionosphere system. These modifica-

tions, while being substantial, do not seem to be, in and of themselves, so drastic as to rule out this transportation system. Historically, whenever man enters a new environment he modifies his culture, technology, and himself, while in turn altering the environment, both by his activities and to suit his needs. The magnetosphere is no exception, and as man becomes more involved in space in the near future, he will begin to modify it.

REFERENCES

1. Solar Systems Concept Definition Study (Exhibit C). SD 78-AP-0115, National Aeronautics and Space Administration, 1978.

2. Kaufmann, Harold R.: Interaction of a Solar Array with an Ion Thruster Due to the Charge-Exchange Plasma. NASA-CR-135099, Annual Report, October, 1976.

3. Carruth, M. R.; and Brady, M. E.: Production of Charge-Exchange Plasma Produced by an Ion Thruster. AIAA 13th Fluid and Plasma Dynamics Conference, Snowmass, Colorado, July 14-16, 1980.

4. Liemohn, H. B.; Holze, D. H.; Leavens, W. M.; and Copeland, R. L.: Ion Thruster Plasma Dynamics near High Voltage Surfaces on Spacecraft. Part of Space Systems and Their Interactions with Earth's Space Environment, ed. by Henry B. Garrett and Charles P. Pike, American Institute of Aeronautics and Astronautics, 1980, pp. 557-598.

5. Parks, D. E.; and Katz, I.: Spacecraft-Generated Plasma Interaction with High Voltage Solar Array. AIAA/DCLR 13th International Electric Propulsion Conference, San Diego, April 25-27, 1978.

6. Scholer, M.: On the Motion of Artificial Ion Clouds in the Magnetosphere. Planet. Space Sci., 18, 977, 1970.

7. Siscoe, G. L.; and N. R. Mukherjee. Upper Limits on the Lunar Atmosphere Determined from Solar-Wind Measurements. J. Geophys. Res., 77, 6042, 1972.

8. Hill, T. W.: Origin of the Plasma Sheet. Rev. Geophys. Space Phys., 12, 379, 1974.

9. Hill, T. W.; and Wolf, R. A.: Solar Wind Interactions. Part of The Upper Atmosphere and Magnetosphere, Studies in Geophysics, National Academy of Sciences, Washington, D.C., 1977, pp. 25-41.

10. Barney, Gerald O.: Experiments and Observations on Polarized Plasma Injection. Phys. Fluids, 12, 2429, 1979.

11. Sellen, Jr., J. M.; and Bernstein, W.: Interaction of Collisionless Plasma Streams with Transverse Magnetic Fields. Phys. Fluids, 977, 1964.

12. Fillip, W. G.: Expansions of an Ion Cloud in the Earth's Magnetic Field. Planet. Space Sci., 19, 1095, 1971.

13. Wickham, M.; and Robertson, S.: Cross Field Injection and Trapping of a Continuous Plasma Beam in a Magnetic Mirror. Plasma Phys., 25, 103, 1983.

14. Curtis, S. A.; and Grebowsky, J. M.: Changes in the Terrestrial Atmosphere-Ionosphere-Magnetosphere System Due to Ion Propulsion for Solar Power Satellite Placement. NASA Tech. Memo 79719, Goddard Space Flight Center, J. Geophys. Res., 85, 1729, 1980.

15. Chiu, Y. T.; Luhmann, J. G.; Schulz, M.; and Cornwall, J. M.: Magnetospheric Effects of Ion and Atom Injections by the Satellite Power System. Space Sciences Laboratory Report No. SSL-80(9990)-1, 1980.

16. Chiu, Y. T.: Fate of Argon-Ion Injection in the Magnetosphere. American Institute of Aeronautics and Astronautics, Inc., 1980.

17. Treumann, R.; Bauer, O. H.; Haerendal, G.; Häusler, B.: Dynamics of Quasi-Neutral Beams. International Symposium on Active Experiments in Space, Alpbach, Austria, May 23-28, 1983.

18. Haerendal, G.; and Sagdeev, R. Z.: Artificial Plasma Jet in the Ionosphere. Adv. Space Res., 1, 29, 1981.

19. Drummond, William E.; and Rosebluth, Marshall N.: Anomalous Diffusion Arising from Microinstabilities in a Plasma. Phys. Fluids, 5, 1507, 1962.

20. Kintner, P. M.; and Kelly, M. C.: Ion Beam Produced Plasma Waves Observed by the $\delta n/n$ Plasma Wave Receivers during the Porcupine Experiment. Adv. Space Res., 1, 107, 1981.

21. Jones, Dyfrig: Xe^{+}-Induced Ion-Cyclotron Harmonic Waves. Adv. Space Res., 1, 103, 1981.

22. Norris, A. J.; Johnson, J. F. E.; Sojka, J. J.; Wrenn, G. L.; Cornilleau-Wehrlin, N.: Perraut, S.; and Roux, A.: Experimental Evidence for the Acceleration of Thermal Electrons by Ion Cyclotron Waves in the Magnetosphere. J. Geophys. Res., 88, 889, 1983.

23. Alexandrov, V. A.; Babev, A. P.; Gaydukov, V. Y.; Loebsky, A. S.; Popov, G. A.; and Romanovsky, Y. A.: Energetic Electron Fluxes Stimulated with Pulsed Injection of Plasma in the Ionosphere. Adv. Space. Res., 1, 141, 1981.

24. Cybulski, Ronald J.; Shellhammer, Daniel M.; Lowell, Robert R.; Domino, Edward J.; and Kotnik, Joseph T.: Results from SERT I Ion Rocket Flight Test. NASA TN D-2718, National Aeronautics and Space Administration, Washington, D.C., March 1965.

25. Spiro, R. W.; Reiff, P. H.; and Maher, Jr., L. J.: Precipitating Electron Energy Flux and Auroral Zone Conductances: An Empirical Model. J. Geophys. Res., 87, 8215, 1982.

26. Mead, G. D.: Deformation of the Geomagnetic Field by the Solar Wind. J. Geophys. Res., 69, 1181, 1964.

27. Vasyliunas, V. M.: Concepts of Magnetospheric Convection. Part of The Magnetospheres of Earth and Jupiter, ed. by V. Formisano, D. Reidel Publ. Co., Dordrecht, Holland, 1975, pp. 179-188.

28. Wolf, R. A.: Ionosphere-Magnetosphere Coupling. Space Sci. Rev., 17, 537, 1975.

29. Harel, M.; Wolf, R. A.; Reiff, P. H.; Spiro, R. W.; Burke, W. J.; Rich, F. J.; and Smiddy, M.: Quantitative Simulation of a Magnetospheric Substorm, 1, Model Logic and Overview. J. Geophys. Res., 86, 2217, 1981.

30. Williams, Donald J.: Ring Current Composition and Sources. Part of Dynamics of the magnetosphere, ed. by S.-I. Akasofu, D. Reidel Publ. Co., Dordrecht, Holland, 1979, pp. 407-424.

31. Freeman, J. W.; Hills, H. K.; Hill, T. W.; Reiff, P. H.; and Hardy. D. H.: Heavy Ion Circulation in the Earth's Magnetosphere. Geophys. Res. Lett, 4, 195, 1977.

32. Akasofu, S.-I.; and Aspens, J. O.: Auroral Effects on Power Transmission Line Systems. Nature, 295, 136, 1982.

33. Freeman, J. W.: International Magnetospheric Plasma Flow. ESA SP-148, Proceedings of Magnetospheric Boundary Layers Conference, 1979.

$$NKT \gtrsim \frac{B^2}{2\mu_0}$$

(a) Vacuum expansion.

$$\frac{MNV^2}{2} \gtrsim \frac{B^2}{2\mu_0}$$
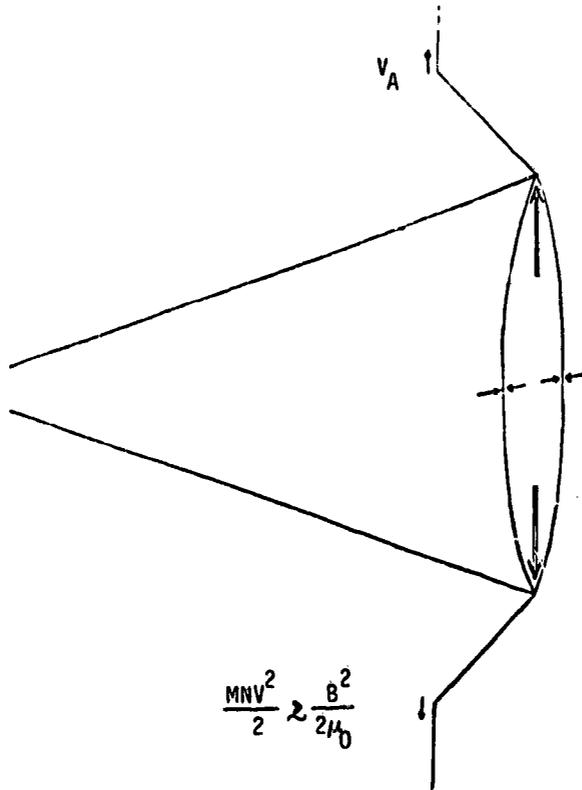
(b) Expansion along $\vec{B}$, also showing Alfven wave propagating down field line.
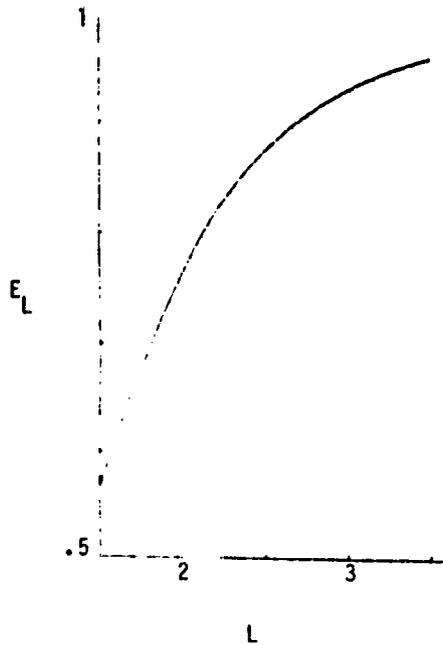
Figure 1. – Two stages of beam expansion.

Figure 2. - Fraction of energy lost to Alfven waves E_L versus magnetic parameter L. It is assumed that e-folding time τ is ~ 10 sec in plasmasphere.
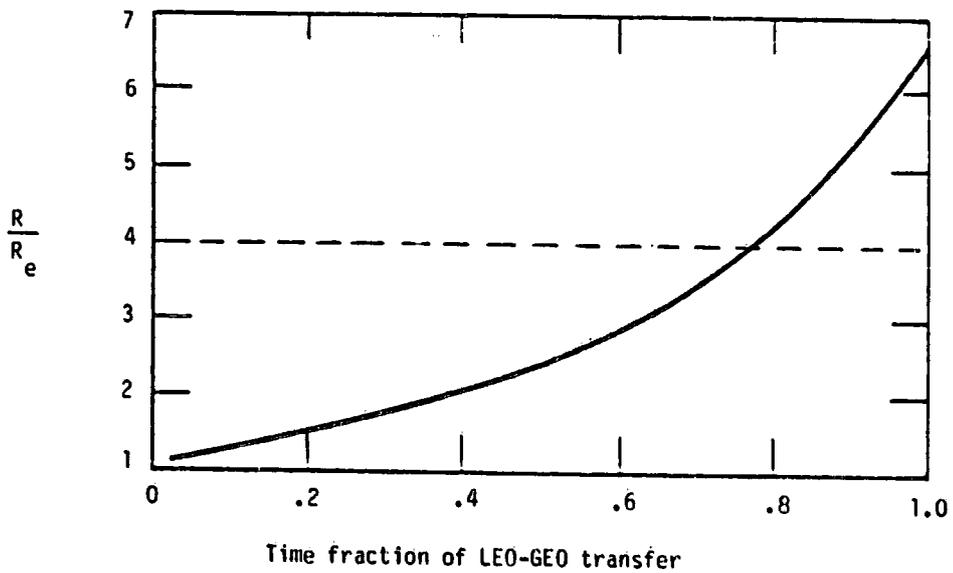

Time fraction of LEO-GEO transfer

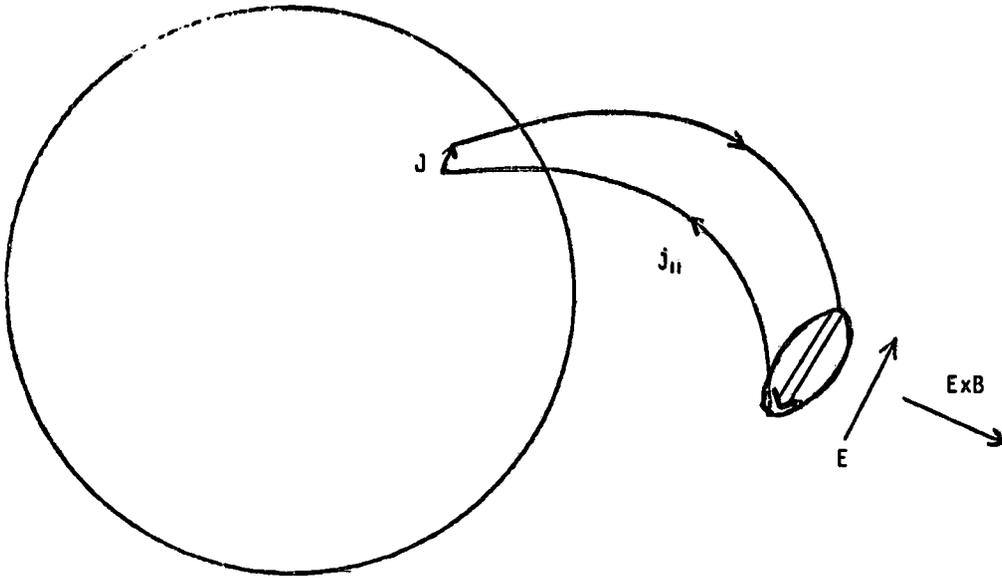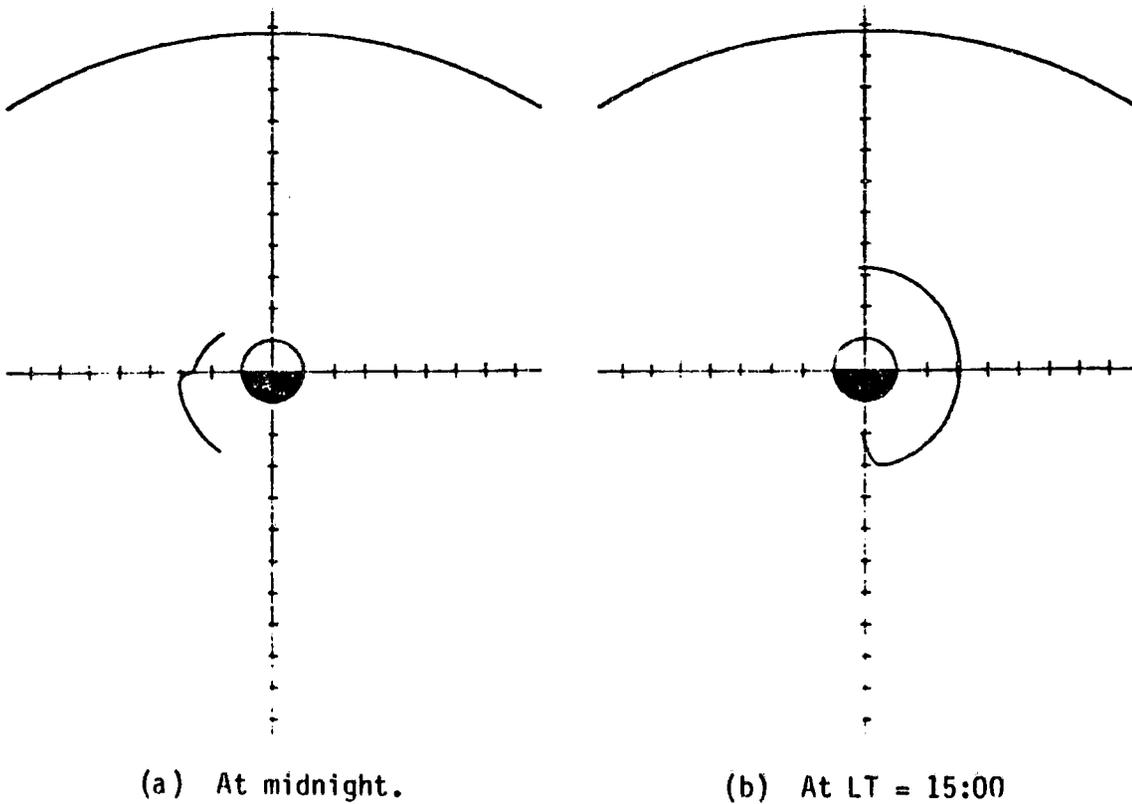Figure 3. - Fraction of total trip time to reach given $R/R_\oplus$. (From Chiu et al. (ref. 15)).

Figure 4. - Birkeland current system for argon flux tube.

(a) At midnight.

(b) At LT = 15:00

Figure 5. - Initial convection path of argon flux tube for beam injection at
L = 2. View is of equatorial plane from above north pole with magnetopause
set at r = 10.8 R$_\oplus$. Σp assumed to be 10 mhos on dayside and 1 mho on
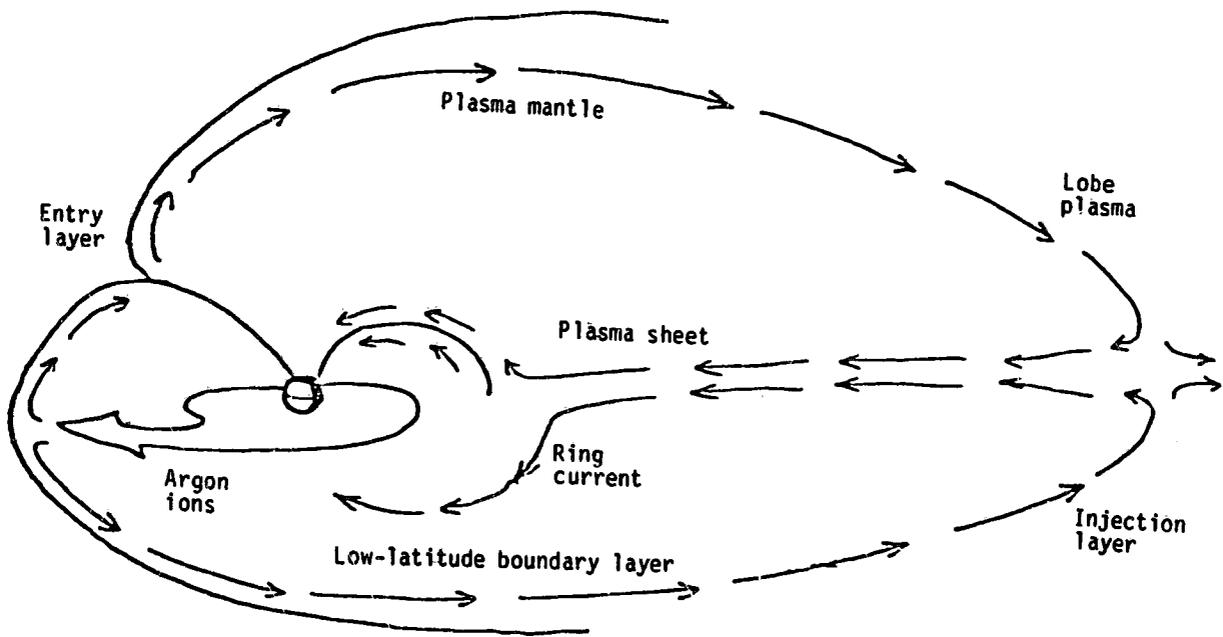nightside. Ticks are in Earth radii.

Figure 6. – Magnetospheric convection of argon. (Adapted from Freeman et al. (ref. 33).)